Experimental Methods for Detecting Entanglement

J. B. Altepeter,* E. R. Jeffrey, and P. G. Kwiat
Department of Physics, University of Illinois at Urbana-Champaign, Urbana, Illinois 61801-3080, USA

S. Tanzilli and N. Gisin†
Group of Applied Physics, University of Geneva, 1211 Geneva 4, Switzerland

A. Acín
ICFO-Institut de Ciències Fotòniques, Jordi Girona 29, Edifici Nexus II, 08034 Barcelona, Spain
(Received 3 February 2005; published 15 July 2005)

Here we present experimental realizations of two new entanglement detection methods: a three-measurement Bell inequality inequivalent to the Clauser-Horne-Shimony-Holt inequality and a nonlinear Bell-type inequality based on the negativity measure. In addition, we provide an experimental and theoretical comparison between these new methods and several techniques already in use: the traditional Clauser-Horne-Shimony-Holt inequality, the entanglement witness, and complete state tomography.

DOI: 10.1103/PhysRevLett.95.033601 PACS numbers: 42.50.Xa, 03.65.Ud, 03.67.Mn

A number of algorithms and protocols have been discovered that exploit quantum mechanics in order to perform tasks which could not be accomplished classically. These include significant improvements in computational complexity for search [1] and factoring [2], advances in cryptography [3], and teleportation of quantum states [4]. These and other protocols make use of the nonclassical nature of the quantum world, epitomized by the phenomenon of entanglement whereby distant systems can exhibit perfectly random yet perfectly correlated behavior. Entanglement has itself been identified as a fundamental resource for quantum computation [5], and its quantification and detection have been the subject of considerable research. In this Letter we present an experimental and theoretical comparison of five methods for entanglement detection, including two which have never before been experimentally realized.

Historically, a violation of Bell's inequality provided the first test for entanglement [6] by measuring a sequence of correlations that could not be explained by any local realistic model. Last year, Collins and Gisin proposed a new type of Bell inequality inequivalent to the traditional Clauser-Horne-Shimony-Holt (CHSH) inequality [7] (inequivalency denotes states that violate one inequality but not the other), requiring measurements in additional bases [8]. While measuring a Bell violation detects entanglement, it does not quantify it nor is it guaranteed to succeed. State tomography [9], in contrast, provides a complete description of a quantum state but requires measurements in even more bases. It was later discovered that it was possible to detect the existence of entanglement without resorting to a violation of local realism. These "entanglement witnesses" [10] proved capable of detecting entanglement using fewer measurements than a tomography, but did not always succeed, sometimes failing to detect a legitimately entangled state. Last year, Yu *et al.* [11] proposed an inequality similar to an entanglement witness, but based on a nonlinear combination of measurement results; it detects *every* entangled state if the correct measurements are chosen.

This Letter describes the preparation of a set of states near the entangled-separable border in Hilbert space and their measurement using the aforementioned entanglement detection techniques. After describing the experimental apparatus used to accomplish this, each of the above detection methods is briefly discussed, followed by an analysis of its experimental implementation. This is, to our knowledge, the first experimental implementation of the inequalities proposed by Collins *et al.* and Yu *et al.*, hereafter referred to as the Geneva and Hefei inequalities, respectively (so named for the cities from which they were proposed). While analyzing each method, it is important to consider the information the test provides (e.g., quantification of entanglement, information about local realism, complete state determination), how many distinct measurement settings are required to perform the test (important if changing bases is experimentally costly), and how the test is affected by both statistical uncertainty and systematic errors (statistical factors primarily determine the time necessary to make a measurement). This Letter concludes with a table quantifying the differences between these methods.

The experiments were carried out using pairs of entangled photons, created via the spontaneous parametric down-conversion of a 351 nm pump beam inside two orthogonally oriented 0.6 mm β-barium borate (BBO) crystals. The optic axes of these crystals were selected such that a horizontal (H) pump beam produces pairs of vertical (V) photons in the first crystal while a vertically polarized pump beam produces pairs of horizontally polarized pairs in the second crystal. Because the crystal spacing and thickness are much shorter than the coherence length of the pump, these processes are coherent, allowing a pump with polarization $\cos(\epsilon)|V\rangle + e^{i\phi}\sin(\epsilon)|H\rangle$ to produce the nonmaximally entangled state

$|\psi(\epsilon,\phi)\rangle = \cos(\epsilon)|HH\rangle + e^{i\phi}\sin(\epsilon)|VV\rangle$ [12]. Additional optical elements [see Fig. 1(a)] allow the creation of a wide range of partially mixed, partially entangled states [13].

The Bell inequality, first proposed in 1964 [6], provides a limit on measurement correlations obtained by any local realistic model. To measure this violation using probabilities measured from separable projectors, we rewrite the CHSH inequality using the convention of [8]:

$$P_{A_1B_1} + P_{A_2B_1} + P_{A_1B_2} - P_{A_2B_2} - P_{A_1} - P_{B_1} \leq 0. \quad (1)$$

Here P_{A_i,B_j} is defined as the probability that photons A and B will be projected into states A_i and B_j, respectively. A violation of the inequality indicates a lack of local realism and the presence of entanglement [14].

If the Bell-type argument is extended to three-measurement bases in each arm ($\{A, B\}_{1,2} \Rightarrow \{A, B\}_{1,2,3}$), it is possible to construct another inequality [8]:

$$P_{A_1B_1} + P_{A_2B_1} + P_{A_3B_1} + P_{A_1B_2} + P_{A_2B_2} + P_{A_1B_3} - P_{A_3B_2} - P_{A_2B_3} - P_{A_1} - 2P_{B_1} - P_{B_2} \leq 0. \quad (2)$$

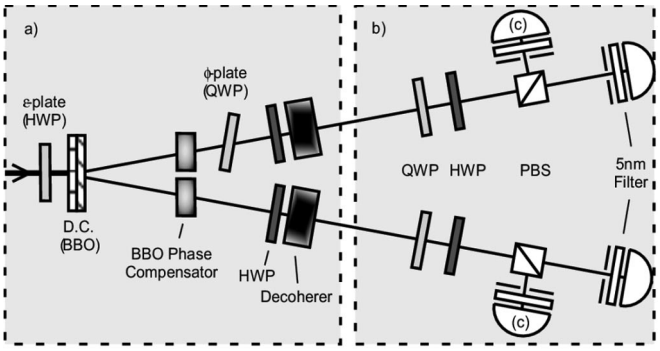

FIG. 1. Experimental setup for the entanglement detection methods discussed. (a) State creation. A 351 nm pump beam down-converts inside two orthogonally oriented 0.6 mm BBO crystals. These crystals are designed such that the superposed down-conversion from both crystals produces the state $\psi(\epsilon,\phi) = \cos(\epsilon)|HH\rangle + e^{i\phi}\sin(\epsilon)|VV\rangle$, where ϵ and ϕ are, respectively, determined by the rotation of the ϵ-HWP (half wave plate) and the tilt of the ϕ-QWP (quarter wave plate) about its optic axis, oriented vertically. Specially designed 245 μm BBO plates compensate for any angular dependence in the phase factor $e^{i\phi}$. Two HWP's transform this state into a state with arbitrary diagonal values in the H/V basis. Finally, two 1 cm decohering quartz crystals destroy all coherence terms in the density matrix except for $|HH\rangle\langle VV|$ and $|VV\rangle\langle HH|$ [19]. (b) Measurement. In each arm, a QWP-HWP-PBS (polarizing beam splitter) combination allows projection into any single-qubit basis. Silicon avalanche photodiodes and coincidence electronics allow the results of separable, two-qubit measurements to be recorded. (c) For some experiments, it is advantageous to add an additional detector at each of the remaining PBS ports, in order to collect not just the results of a single separable projector, but an entire four-element basis measurement.

What is most interesting about this Geneva inequality is that it is *inequivalent* to the CHSH inequality; there exist states that violate the Geneva inequality but do not violate the CHSH inequality and vice versa.

In order to experimentally show this difference, we prepared a class of states which lie on the border of violating the CHSH inequality, within a very small region of Hilbert space. These states are of the form [8]

$$\rho_{CG}(\theta) = \lambda|\psi(\theta,0)\rangle\langle\psi(\theta,0)| + (1-\lambda)|HV\rangle\langle HV|. \quad (3)$$

For each state $\rho_{CG}(\theta)$, λ is chosen such that the CHSH violation of $\rho_{CG}(\theta)$ is theoretically predicted to be exactly equal to 0. These states range from pure to mixed and from entangled to separable, and together exemplify the inequivalency between the Geneva and the CHSH inequalities [see Fig. 2(a) for experimental results].

The primary advantage of either the CHSH or the Geneva inequality is its function as a test of local realism. Both require previous knowledge of the state in order to choose measurement settings that maximize the value of the inequalities. In the CHSH case, a simple analytic proscription has been found [15]; for the Geneva inequality, we used a numerical search.

Note also that both inequalities require probabilities to calculate a violation, but experimentally we measure coincidence rates. In order to transform coincidence rates into probabilities, at least one complete basis is measured; by summing the rates for a complete set of orthonormal projectors we obtain an estimate of the intensity of incident states, allowing us to transform any coincidence rate into a probability. Probabilities involving only one projection (e.g., P_{A_1}) are reconstructed by summing other terms (e.g., $P_{A_1,B_X} + P_{A_1,B_X^\perp}$, where B_X can be any projector).

Our third detection method is the entanglement witness [10]. An entanglement witness, denoted by W, is a Hermitian nonpositive operator whose overlap with product states is non-negative, i.e., for any separable state $|\alpha\beta\rangle$, $\langle\alpha\beta|W|\alpha\beta\rangle \geq 0$. Entanglement witnesses detect more states than a Bell inequality (for each entangled two-qubit state, there exists a witness that can detect its entanglement [10]), using fewer measurements than a full tomography, but requiring a witness suited for a given entangled state. Here we construct a witness that is capable of detecting the entanglement for all $\rho_{CG}(\theta)$.

Consider the spectrum of the partial transposition [5,15] ρ^{T_A} of the state $\rho_{CG}(\theta)$. Denote by $\lambda_{\min}(\theta)$ its minimum eigenvalue and by $|e_n(\theta)\rangle$ the corresponding eigenvector. Since $\rho_{CG}(\theta)$ is entangled when $0 < \theta < \pi$, $\lambda_{\min}(\theta)$ is negative in the same range [15] (the value of this eigenvalue is linearly related to the negativity). Moreover, $|e_n(\theta)\rangle$ turns out to be independent of θ, so $|e_n(\theta)\rangle = |e_n\rangle$. It follows that $W = |e_n\rangle\langle e_n|^{T_A}$ is an entanglement witness, with $\mathrm{Tr}[W\rho] \geq 0$ for all separable states and less than zero for all $\rho_{CG}(\theta)$. It is possible, using local measurements, to estimate the value of $\mathrm{Tr}[W\rho]$ [16].

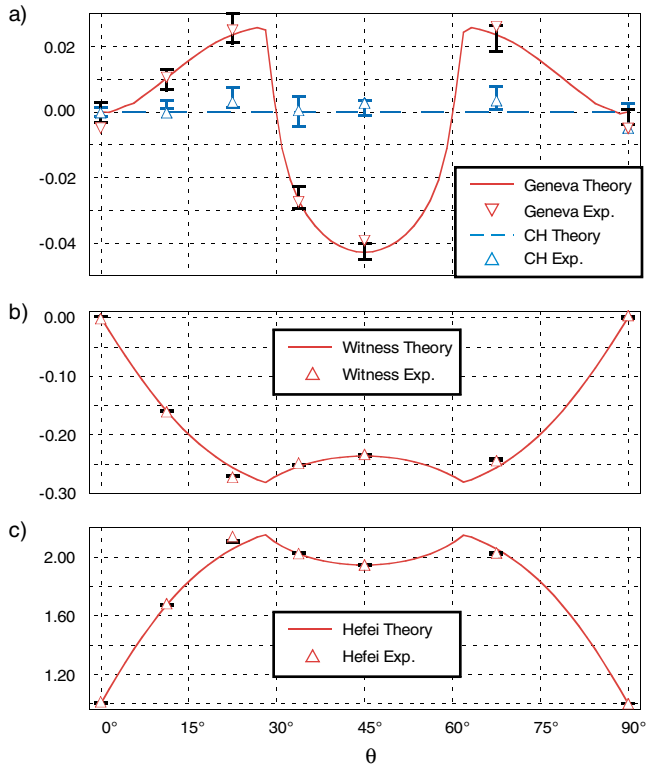

FIG. 2 (color online). Experimentally measured values for four different entanglement detection methods, each applied to the same set of states. These states were all of the form $\rho_{CG}(\theta)$ [see Eq. (3)]. In all cases the solid lines represent theoretical values for ideal states, calculated numerically. In practice, the experimental states deviated slightly from the exact form of ρ_{CG}. (They all maintained >99% fidelity with the target.) The error bars indicate the *state tomography's* $1-\sigma$ error region for these experimentally created states, and so for outliers may fail to bound the experimentally measured violations. (a) Measured violations of the Geneva and CHSH inequalities, which are manifestly inequivalent. ρ_{CG} is intentionally constructed so that the theoretical value of the CHSH violation is always exactly zero. Both the CHSH and Geneva inequalities have been renormalized so that 0 represents the border between a violation and nonviolation. The renormalized range of the Geneva inequality is -2 to 0.25 and the range of the CHSH inequality is -1 to $\frac{(2\sqrt{2}-2)}{4}$. (b) Experimentally measured values for an entanglement witness based on the negativity. Negative values indicate entanglement. (c) Experimentally measured values of the Hefei inequality, a nonlinear Bell-type inequality based on the negativity. Because of the curves' fundamental similarity, the value of 2(c) is equal to 1 minus 4 times 2(b).

Figure 2(b) shows the results of this estimation, using the states $\rho_{CG}(\theta)$.

While entanglement witnesses are based on the linear overlap between a density matrix and an operator, it is possible to construct *nonlinear* inequalities based on the same types of measurements. Consider two sets of mutually complementary observables, $\{A_i\}$ and $\{B_i\}$, having identical orientation ($A_1A_2A_3 = B_1B_2B_3$). The Hefei Group proved [11] that a two-qubit state is separable if and only if

$$\sqrt{\langle A_1B_1 + A_2B_2\rangle_\rho^2 + \langle A_3 + B_3\rangle_\rho^2} - \langle A_3B_3\rangle_\rho \leq 1 \qquad (4)$$

for all A_i, B_i where $\langle O\rangle_\rho = \mathrm{Tr}[\rho O]$. Moreover, the maximal value of the above inequality is equal to $1 - 4\lambda_{\min}$ with $\lambda_{\min}$ equal to the minimal eigenvalue of the partial transpose of the density matrix.

The results of the measurement of this Hefei inequality—which once again requires one to choose the correct measurement bases to match the state—are shown in Fig. 2(c). The y axis in Fig. 2(c) shows the value of the violation: a value greater than one indicates entanglement, and a value of three can be obtained only by a maximally entangled state.

All four of the entanglement detection methods already discussed share two disadvantages: they require previous knowledge of the state to be effectively applied, and they fail to quantify the *amount* of entanglement present. These problems can be overcome by taking a complete quantum state tomography (QST), which through a series of separable measurements reconstructs the full density matrix. While QST requires no prior knowledge of the state and allows any of the above quantities to be derived from the density matrix, it does not necessarily provide a test of local realism [17] and it requires a minimum of 16 separable measurement settings [9,18].

While 16 measurements are the minimum necessary for QST, it is possible to instead use a set of 36 measurements composed of nine complete bases. Surprisingly, the information provided from these additional measurements is sufficient to *reduce* the total time required for QST for a given precision (using our experimental system) by as much as a factor of 3. If, in addition, every two-qubit state is projected into one of four orthogonal projectors, this can be reduced by a further factor of 4, as only nine measurements are necessary [see Fig. 1(c)].

This reduction in experimental time underscores two distinct and often competing measures of an entanglement detection method's efficiency. The first is the number of different measurements necessary, important because of the time it takes to switch between measurements. For our automated system, where different measurement settings correspond to different wave plate orientations, this is usually a minor factor. The second consideration is the total number of state copies required—linearly related to the total measurement time.

Table I shows the number of measurements and the total number of state copies *per measurement* necessary to accurately measure, using each method, four representative two-qubit states: $I/4$, $\rho_{CG}(\frac{\pi}{8})$, $|\psi^+\rangle = \frac{1}{\sqrt{2}}(|HH\rangle + |VV\rangle)$, and $|HH\rangle$. The number of measurements were minimized in each case, which for the 2-detector case leads to a far larger necessary ensemble size, exemplified by the factor

TABLE I. This table compares five different entanglement detection methods using two different experimental configurations. For each detection method, the second column (M#) indicates the number of necessary measurement settings. Each additional column shows, for each of four two-qubit states, the minimum number of distinct two-qubit systems that need to be used, *per measurement*, in order to attain a $\pm 1\%$ statistical error. Here, a $\pm 1\%$ error is measured relative to the entire range of the measured quantity. For example, the CHSH inequality ranges from -1 to ~ 0.207, making a $\pm 1\%$ error equal to a $\pm 0.01 \times 1.207$ error in the violation. The minimum state copies necessary were numerically estimated using a Monte Carlo simulation of the expected data, the results of which corresponded to analytic estimates. The third through sixth columns, respectively, show the state copies per measurement necessary for the states $I/4$, $\rho_{CG}(\frac{\pi}{8})$, $|HH\rangle$, and $|\psi^+\rangle = \frac{1}{\sqrt{2}}(|HH\rangle + |VV\rangle)$. (a) Results for a single projector (2-detector) setup, where each two-qubit state is measured using only a single separable two-qubit projector. (b) Results for a full basis measurement (4-detector) setup, where each two-qubit state is measured simultaneously by four mutually orthogonal projectors [see Fig. 1(c)].

(a) Single projector/two detectors

Method	M#	$I/4$	$\rho_{CG}(\frac{\pi}{8})$	ψ^+	$\|HH\rangle$
CHSH	7	6800	4400	12400	200
Geneva	11	7000	5400	2600	200
Ent. witness	8	800	400	200	500
Hefei	8	12 300	2500	400	200
Tomography[a]	16	23 500	8800	900	900

(b) Four projectors/four detectors

Method	M#	$I/4$	$\rho_{CG}(\frac{\pi}{8})$	ψ^+	$\|HH\rangle$
CHSH	4	3400	1000	2100	200
Geneva	8	2300	2200	1600	200
Ent. witness	3	800	400	200	500
Hefei	3	5500	1600	400	100
Tomography[a]	9	4000	1500	400	200

[a]Tomography returns a density matrix, from which the results of each other test can all be derived. The tomography entries in this chart show the minimum state copies necessary to attain a density matrix precise enough to reduce the error on each of these derived quantities to less than $\pm 1\%$.

of $2.6 \approx ([8800 \times 16]/[1500 \times 9 \times 4])$ increase in necessary state copies between 36 and 16 measurement, 2-detector tomographies of $\rho_{CG}(\frac{\pi}{8})$.

These results are a numerical upper bound that is highly dependent not only on the state to be measured, but the particular measurement *settings* that are chosen (for any given state there may be many equivalent ways to measure a maximal violation). This is exemplified by the 2-detector CHSH results for $|\psi^+\rangle$, which appear to be quite high, and $|HH\rangle$, which are quite low. The maximally entangled state requires very specific measurements, and leaves little freedom to optimize for low errors. The violation for $|HH\rangle$, however, is theoretically zero, allowing measurement settings to be chosen that are all orthogonal to $|HH\rangle$, all resulting in probability zero, and all with low errors.

Comparing these five methods, we find that the CHSH and Geneva inequalities are useful for performing tests of local realism, the Hefei inequality and the entanglement witness can be used to quickly bound $\lambda_{\min}$, and the tomography appears to be the most attractive option in general; each other method first *requires* a tomography to choose its measurement settings—a tomography that can be used to derive any information about a state. In the 4-detector case, the tomography actually *outperforms* several other methods for entangled states, the states most likely to be measured using entanglement detection techniques.

This work was supported by the National Science Foundation (Grant No. EIA-0121568) and the MURI Center for Photonic Quantum Information Systems (ARO/ARDA program DAAD19-03-1-0199).

*Electronic address: altepete@uiuc.edu
†Electronic address: Nicolas.Gisin@physics.unige.ch

[1] L. K. Grover, Phys. Rev. Lett. **79**, 325 (1997).
[2] P. W. Shor, in *Proceedings of the 35th Annual Symposium on Foundations of Computer Science*, edited by S. Goldwasser (IEEE Computer Society Press, Los Alamitos, CA, 1994), p. 116.
[3] N. Gisin, G. Ribordy, W. Tittel, and H. Zbinden, Rev. Mod. Phys. **74**, 145 (2002).
[4] C. H. Bennett *et al.*, Phys. Rev. Lett. **70**, 1895 (1993).
[5] M. A. Nielsen and I. L. Chuang, *Quantum Computation and Quantum Information* (Cambridge University Press, Cambridge, U.K., 2000).
[6] J. S. Bell, Physics (Long Island City, N.Y.) **1**, 195 (1964).
[7] J. F. Clauser, M. A. Horne, A. Shimony, and R. A. Holt, Phys. Rev. Lett. **23**, 880 (1969).
[8] D. Collins and N. Gisin, J. Phys. A **37**, 1775 (2004).
[9] A. G. White, D. F. V. James, P. H. Eberhard, and P. G. Kwiat, Phys. Rev. Lett. **83**, 3103 (1999).
[10] M. Lewenstein, B. Kraus, J. I. Cirac, and P. Horodecki, Phys. Rev. A **62**, 052310 (2000).
[11] S. Yu, J.-W. Pan, Z.-B. Chen, and Y.-D. Zhang, Phys. Rev. Lett. **91**, 217903 (2003).
[12] A. G. White, D. F. V. James, W. J. Munro, and P. G. Kwiat, Phys. Rev. A **65**, 012301 (2002).
[13] T.-C. Wei *et al.*, Phys. Rev. A (to be published).
[14] J. F. Clauser and M. A. Horne, Phys. Rev. D **10**, 526 (1974).
[15] M. Horodecki, P. Horodecki, and R. Horodecki, Phys. Lett. A **223**, 1 (1996).
[16] O. Gühne *et al.*, J. Mod. Opt. **50**, 1079 (2003).
[17] It is possible for tomography data that is explainable by a local hidden variable model to predict an entangled state that *could* violate local realism.
[18] J. B. Altepeter, D. F. V. James, and P. G. Kwiat, *Quantum State Estimation*, Lecture Notes in Physics (Springer, Berlin, 2004).
[19] P. G. Kwiat, A. J. Berglund, J. B. Altepeter, and A. G. White, Science **290**, 498 (2000).